

Physiology in Fractal Dimensions: Error Tolerance

Bruce J. West

Department of Physics
University of North Texas
Denton, Texas 76203

The natural variability in physiological form and function is herein related to the geometric concept of a fractal. The average dimensions of the branches in the tracheo-bronchial tree, long thought to be exponential, are shown to be an inverse power law of the generation number modulated by a harmonic variation. A similar functional form is found for the power spectrum of the QRS-complex of the healthy human heart. These results follow from the assumption that the bronchial tree and the cardiac conduction system are fractal forms. The fractal concept provides a mechanism for the morphogenesis of complex structures which are more stable than those generated by classical scaling (i.e., they are more error tolerant).

Keywords—Fractals, Lungs, Heart, Scaling, Error tolerance.

1. INTRODUCTION

Early in this century D'Arcy Thompson explored problems of scale, size, and shape in the natural sciences (9). He developed the idea that biological processes have underlying physical constraints which led him to the formulation of several important scaling relations in biology—describing (e.g., how proportions tend to vary as an animal grows. His approach relied on a key assumption, namely, that biological processes, like their physical counterparts, are continuous, homogeneous, and regular). Observation and experiment, however, suggest the opposite. Most biological systems, and many physical ones, are discontinuous, inhomogeneous, and irregular (6,2). Thus, physiologists, have been led to ask questions of the kind: “Is there a characteristic scale factor that governs the decrease in mean bronchial measure from the trachea to the terminal bronchioles?”; “Does the type of architecture seen in the pulmonary tree share any basic morphogenetic link with branching networks in the heart, vascular tree, kidney, and liver?”; “Is regular sinus rhythm really regular—does it have a characteristic scale of time?”.

Questions like these, which have been of traditional interest in biology, can now be addressed using concepts developed in *nonlinear dynamics systems theory*. As its name suggests, this discipline is concerned with systems whose output is not a linear function of its input. Nonlinear relations are the rule in biology, both in dynamic processes and in static structures. In this discussion we are primarily concerned with

Address correspondence to Bruce J. West, PhD, Department of Physics, University of North Texas, P.O. Box 5368, Denton, TX 76203.

the role of static structure in physiology, and how the description of that structure has changed since Thompson first introduced the classical scaling concept of similitude (13).

A significant contribution to the study of nonlinear form and function was made by the development of the mathematical concept of *fractals*. Since its introduction in the last decade, the fractal concept has already permeated the physical sciences, with applications to the study of turbulence, meteorology, astronomy, magnetization, and polymer chemistry, to name but a few (6). The first papers discussing fractals in a biomedical context have only recently appeared, and so herein we spend some time developing the background in this relatively new field, focusing on our incipient efforts to apply nonlinear analysis and fractal constructs to physiology and medicine (2,14,5).

2. WHAT IS A FRACTAL?

The term “fractal” refers to objects (processes) that are characterized by a fractional dimension. It should be pointed out that operationally there are three different uses of the term fractal: geometrical, statistical, and correlational. The geometry of Euclid is concerned with continuous lines and simple smooth forms that uniformly fill spaces of integer dimensions. These static forms of classical geometry are found almost nowhere in nature, being as they are the result of human intellect and machinery. In Fig. 1 we contrast a few examples of geometric solids with a typical pattern arising in nature. The branching pattern could be the root system of a bush, a static discharge leading to the breakdown of a dielectric, or any of a number of other physical or biological phenomena. The main difference between the two types of objects is that the classical ones have well defined heights, widths, and depths, whereas the fractal one does not. If one were to magnify the surface of a Euclidean object it would appear at some scale to be smooth and regular. On the other hand, the irregular structure of an ideal fractal object appears no smoother under magnification than it does full size. At each level of magnification more and more structure is revealed; the ir-

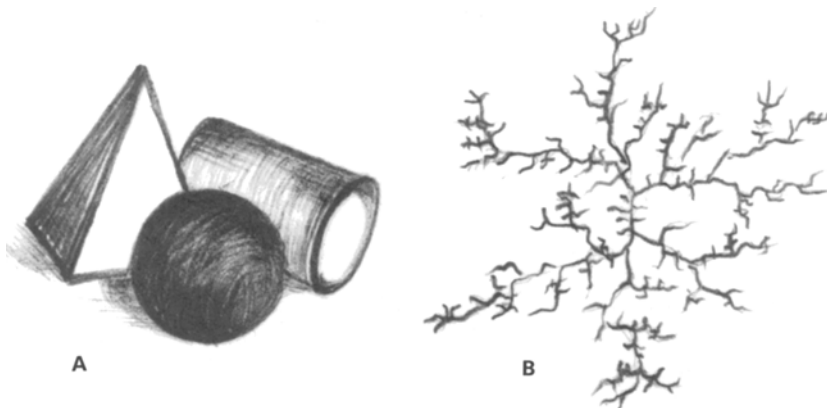


FIGURE 1. Examples of smooth continuous Euclidean objects are shown in 1A. A typical natural object that does not have a classical description, i.e., a fractal, is shown in 1B.

regular structure that is uncovered is a function of the magnification. Said differently, if one were to measure the length of one of the tendrils depicted in Fig. 1b, its length would depend on the size of the measuring instrument. In the limit that the ruler becomes infinitesimally small, the length of the tendril becomes infinitely long. This dependence of the size of the object on the measuring instrument is one of the defining properties of a fractal (6).

A second example of a fractal is that of a curve treated as a geometric object. In Fig. 2 we construct such a fractal curve from the superposition of a number of independent Fourier components. We begin with a mode having a fundamental frequency Ω_0 , and a unit amplitude, and add to it a second periodic term of frequency $b\Omega_0$, with amplitude $1/a$, and to these add a third periodic term of frequency $b^2\Omega_0$, with amplitude $1/a^2$, and so on [cf. Fig. 2a]. The resulting function is an infinite series of periodic terms, each term of which has a frequency that is a factor b larger than the preceding term and an amplitude that is a factor of $1/a$ smaller. The curve generated by this function is depicted in Fig. 2b. At first glance, this curve would seem to be a ragged line with many abrupt changes in direction. If we now magnify a small region of the line, as in the second drawing (Fig. 2b), we see that the enlarged region appears qualitatively the same as the original curve. If we now magnify a small region of this new line, as in the third drawing, we again obtain a curve that is qualitatively indistinguishable from the first two. This is the property of "self-similarity" (13).

The German mathematician Karl Weierstrass was the first to give these ideas a mathematical form. A generalization of the Weierstrass function was first suggested by Lévy and later extensively discussed by Mandelbrot and subsequently by Berry and Lewis (1):

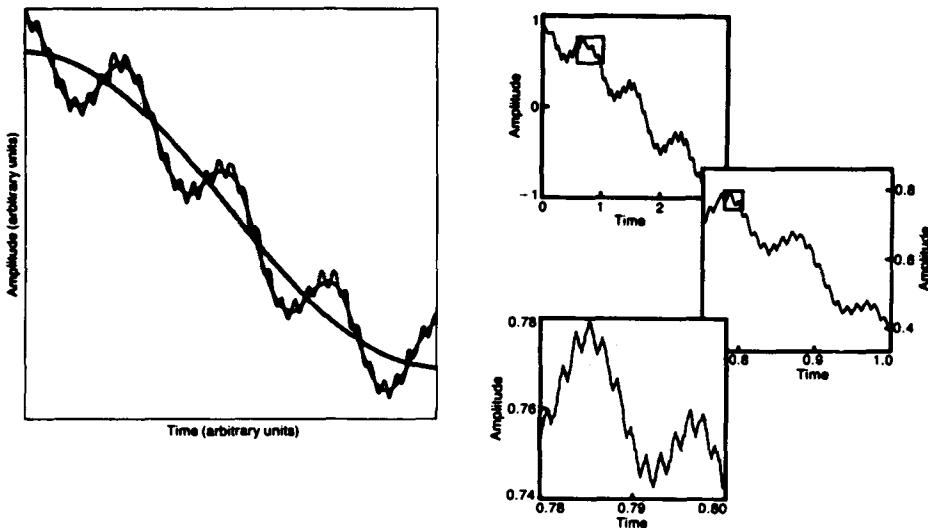


FIGURE 2. A line is constructed from the Weierstrass function with $a = 4$, $b = 8$ and $\Omega_0 = 1$. In 2A, the separate contributions of the Fourier series to the line is depicted. In 2B, various regions of the final are magnified to illustrate its "self-similarity" [from West and Goldberger (3)].

$$W(t) = \sum_{n=-\infty}^{\infty} \frac{1}{a^n} [1 - e^{ib^n \Omega_0 t}] e^{i\phi_n}, \quad (2.1)$$

where the phase ϕ_n is an arbitrary real constant. The Weierstrass function was the first explicit representation of a continuous function that is nowhere differentiable, and appears to be the first example of a fractal function. Thus, we see that because the generalized Weierstrass function (2.1) has no smallest period, i.e., the period $1/b^n \Omega_0 \rightarrow 0$ as $n \rightarrow \infty$, it consists of a superposition of smaller and smaller wiggles. The degree of irregularity is determined by the fractal dimension of the curve. This dimension is greater than the topological dimension of the curve which is unity, but smaller than the Euclidean dimension of the plane which is two. Thus, for a fractal curve of dimension D we must have $1 < D < 2$. To calculate D we examine some of the mathematical properties of a fractal function.

The self-similarity property of the above curve can be observed directly from (2.1) by reorganizing the terms in the series for $\phi_n = 0$ to obtain:

$$W(t) = 1/a W(bt), \quad (2.2)$$

which has the solution:

$$W(t) = At^\mu, \quad (2.3)$$

where A is constant and μ is determined by direct substitution to be:

$$\mu = \ln a / \ln b. \quad (2.4)$$

The fractal dimension D for the curve generated by (2.1) with $\phi_n = 0$ is given by $2 - D = \mu$ [cf. (2.4)] so that:

$$D = 2 - \ln a / \ln b, \quad (2.5)$$

which for the parameter values used in Fig. 2, $a = 4$ and $b = 8$, is $D = 1.333$.

Thus, geometrical fractals are families of shapes containing infinite levels of detail. On smaller and smaller scales, the intrinsic structure is similar to that of the larger form, a property called self-similarity. As the fractal dimension increases from one to two, more and more detail is generated in planar structures. The same is true as the fractal dimension decreases between three and two. An apparently solid, three-dimensional, object becomes more and more "surface-like" as the dimension decreases, as in the case of the lung that we discuss subsequently.

The set of phases $\{\phi_n\}$ may be chosen deterministically as we did above, or randomly as we do now to generate a statistical fractal. If ϕ_n is a random variable uniformly distributed on the interval $(0, 2\pi)$, then each choice of the set of values $\{\phi_n\}$ constitutes a member of an ensemble for the statistical function $W(t)$. If the phases are also independent as $b \rightarrow 1^+$, then $W(t)$ is a Gaussian random variable. The condition $1 < D < 2$ is required to ensure the convergence of the sum (2.1).

Consider the increment in $W(t)$,

$$\begin{aligned} \Delta W(t, T) &= W(t + T) - W(t) \\ &= \sum_{n=-\infty}^{\infty} \frac{1}{b^{n(2-d)}} [1 - e^{ib^n \omega_0 T}] \exp[ib^n \Omega_0 t + i\phi_n] \end{aligned} \quad (2.6)$$

and assume that the ϕ_n are independent random variables uniformly distributed on the interval $(0, 2\pi)$. The mean square increment:

$$\begin{aligned} C(T) &= \langle |\Delta W(t, T)|^2 \rangle_{\phi} \\ &= \sum_{n=-\infty}^{\infty} \frac{2}{b^{n(4-l)}} [1 - \cos(b^n \Omega_0 T)] \end{aligned} \quad (2.7)$$

where the ϕ subscript on the brackets denotes an average over an ensemble of realizations of the ϕ_n -fluctuations. The righthand side of (2.7) is independent of t (i.e., it depends only on the difference T , so that $\Delta W(t)$ is a stationary random process).

Note that (2.7) has the same form as the real part of the extended Weierstrass function (2.1) when $\phi_n = 0$. If we shift the summation index in (2.7) by unity we obtain the scaling relation (1):

$$C(bT) = b^{2(2-D)} C(T), \quad (2.8)$$

which is of the same form as (2.2) with $a^2 = b^{2(2-D)}$ [cf. (2.5)]. Thus, we see that the correlations of the extended Weierstrass function, like the function itself, is self-affine. Here again the solution to the renormalization group relation is a modulated inverse power law:

$$C(T) = BT^{2\mu}, \quad (2.9)$$

where again μ has the value given by (2.4).

The dynamic process described here has a multiplicity of time scales that are manifest in a power spectrum with a broad profile of response times. One discovers that the process in question shows structures (fluctuations) over multiple orders of temporal magnitude, e.g., minutes to milliseconds in such physiological processes as say the heart beat, in the same way that fractal forms exhibit detail over several orders of spatial magnitude in such physiological structures as the lung (2). Consider the Fourier transform of (2.9) from which we obtain the power spectrum:

$$S(\omega) = \int_{-\infty}^{\infty} e^{-i\omega t} C(t) dt = \frac{B}{\omega^{2\mu+1}}, \quad (2.10)$$

where B is assumed to be a constant. A fractal scaling between variations of different time scales lead to a frequency spectrum having the inverse power-law distribution (2.10).

The key feature of the geometrical, statistical, and temporal fractals is the *lack of a fundamental scale*. There is no minimal unit of length in the geometric case, each size varies inversely with the measuring scale. Similarly, there is no fundamental period in the time domain. Perhaps the most subtle is the lack of scale for stochastic

processes, which implies that the random fluctuations in the statistical process are the same on all scales.

The above examples illustrate three related properties of fractal forms: *self-similarity*, *heterogeneity*, and the *absence of a characteristic scale*. These geometric features are characteristic of a variety of seemingly unrelated biological forms: the tracheo-bronchial tree, the His-Purkinje conduction system of the heart, the chordae tenineae, the biliary network, the vascular tree, and the urinary collecting system to name a few. The fractal dimension D has proven to be a useful way to characterize the geometric and/or dynamic structure of a number of these biological systems.

3. PHYSIOLOGY IN FRACTAL DIMENSIONS

To firmly fix these ideas, let us consider the human lung as a paradigm of biological complexity. We see from the plaster cast (Fig. 3) that a human lung has two dominant features, organization along with irregularity and richness of structures, both

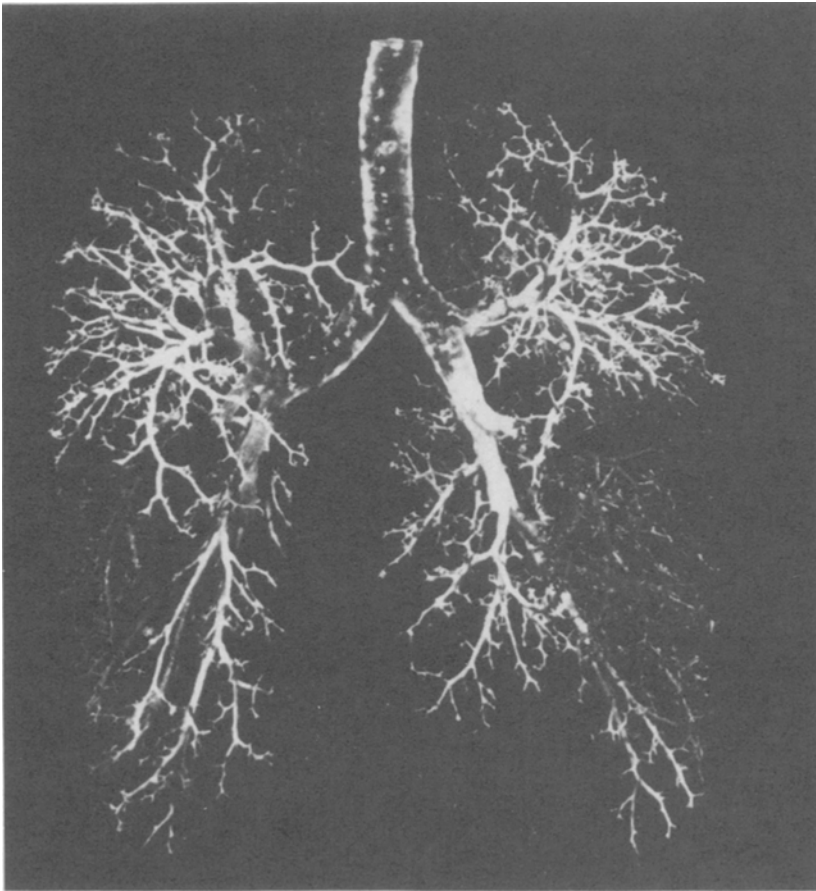


FIGURE 3. The plaster cast of a human lung is depicted [from West and Goldberger (13)].

of which are required to perform the gas exchange function for which the lung is designed. The plaster cast suggests that the lung may have the properties of heterogeneity, self-similarity (over some range of scales) and the lack of a smallest scale.

Before exploring the implications of assuming the lung is a fractal structure, let us review the classical model of the mammalian lung. Consider the number of branches emanating from the trachea. If z is the generation number, then since there are two stems leaving each vertex, there is a geometric increase in the number of branches (i.e., $N(z) = 2^z N(0)$). This simple scaling argument was used to determine the size of the airways. It was assumed by Weibel and Gomez (10) that the diameter of an airway scaled as $d(z) = qd(z - 1)$ between successive generations. This scaling assumption led to an exponential decrease in the size of the diameter. For the first ten generations the average diameter of the airway in the human lung seems to satisfy the exponential relation, $d(z) = d(0)e^{-\Gamma z}$ where $\Gamma = \ln(1/q)$ with $q < 1$. Subsequently, there is a marked deviation from this exponential form (Fig. 4) where $\ln d(z)$ versus z is depicted. Weibel and Gomez assume that a new diffusive mechanism is initiated at $z = 10$ and this mechanism leads to a second exponential. We wondered if in fact

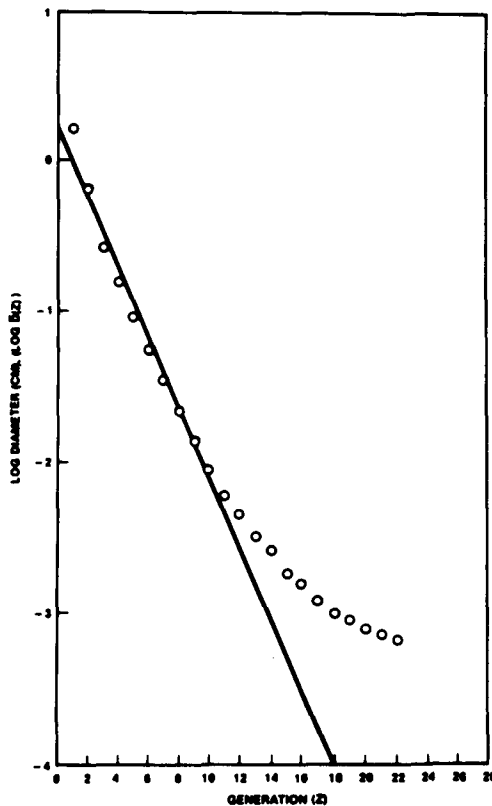


FIGURE 4. The data of Weibel and Gomez (10) (o) is compared with the prediction of the classical scaling model (—).

there is a better fit to the data that does not require the introduction of this second mechanism (12).

We replot the Weibel-Gomez data on log-log graph paper and observe that there appears to a dominant inverse power-law behavior in the average diameter with z . This dominant behavior is observed in (Fig. 5) and is not just characteristic of humans, but is also observed in dogs, rats and hamsters. In all of these data sets there appears to be a harmonic variation of the data points around the inverse power-law curve. In order not to anticipate the fit of the fractal model to the data we defer discussion of the fit until we have developed the fractal theory (12).

The first question to ask before applying the fractal idea is what has been omitted in the classical scaling argument that might possibly account for the inverse power-law behavior and the harmonic variation of the average size of an airway. The property that has been neglected in the *theoretical* discussions is the multiplicity of scales present in each generation of the bronchial tree. If we denote these scales by Γ then $d(z)$ in fact becomes $d(z, \Gamma)$ and the quantity being graphed has been averaged over the Γ -scales:

$$\langle d(z) \rangle = \int_0^\infty p(\Gamma) d(z, \Gamma) d\Gamma. \quad (3.1)$$

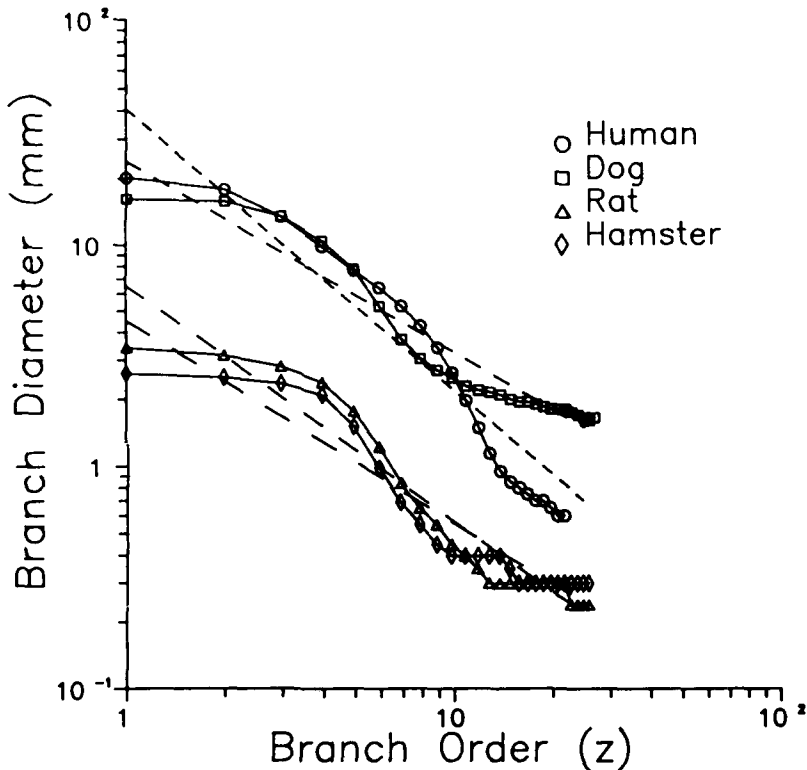


FIGURE 5. The data from Raabe *et al.* (8) for the average diameter of the mammalian lung is compared with the predictions of the fractal (renormalization) lung model of West *et al.* (12).

The distribution of scales $p(\Gamma)$, in part, determines the functional form of the average diameter $\langle d(z) \rangle$. The quantity $p(\Gamma)d\Gamma$ is the probability that a particular scale in the interval $(\Gamma, \Gamma + d\Gamma)$ is present in the measured diameter. Weibel and Gomez implicitly use $p(\Gamma) = \delta(\Gamma - \Gamma_0)$, i.e., a single scale to characterize the bronchial tree which, as we have seen, results in the exponential form of $\langle d(z) \rangle$. We must determine the form of $p(\Gamma)$ in the general case to determine how $\langle d(z) \rangle$ differs from the exponent form.

Rather than prescribing a particular functional form of the probability density, West et al. (12) formulated an argument based on scaling of the parameter Γ . Consider a distribution having a finite central moment, say a mean value $\bar{\Gamma}$. Now, following Montroll and Shlesinger (7), we apply a scaling mechanism such that $p(\Gamma)$ has a new mean value $\bar{\Gamma}/b$:

$$p(\Gamma, \bar{\Gamma}) \rightarrow p(\Gamma, \bar{\Gamma}/b) \tag{3.2}$$

and we assume this occurs with relative frequency $1/a$. We apply the scaling again so that the scaled mean is $\bar{\Gamma}/b^2$ and occurs with relative frequency $1/a^2$. This scaling process is repeated again and again and eventually generates the distribution:

$$P(\xi) \propto p(\xi) + \frac{1}{a} p(b\xi) + \frac{1}{a^2} p(b^2\xi) + \dots \tag{3.3}$$

where we have introduced the dimensionless variable $\xi = \Gamma/\bar{\Gamma}$. Thus using (3.3) to evaluate the average diameter we obtain:

$$\langle\langle d(z) \rangle\rangle \propto \langle d(z) \rangle + \frac{1}{a} \langle d(z/b) \rangle + \frac{1}{a^2} \langle d(z/b^2) \rangle + \dots \tag{3.4}$$

where the double bracket denotes the average with respect to the distribution (3.3). Introducing the normalization constant C given by:

$$\int_0^\infty P(\xi)d\xi = C(a, b) \tag{3.5}$$

the series (3.4) can be written in the more compact form:

$$\langle\langle d(z) \rangle\rangle = \frac{1}{a} \langle\langle d(z/b) \rangle\rangle + C(a, b) \langle d(z) \rangle \tag{3.6}$$

as the number of terms in the series becomes infinite.

We note the renormalization group relation (RG) (3.6) that results from this argument (4). Here we restrict our attention to the dominant behavior of the solution to this RG relation. If we separate the contributions to $\langle\langle d(z) \rangle\rangle$ into that due to singularities, denoted by $d_s(z)$, and that which is analytic, then the singular part of (3.6) satisfies the functional equation:

$$d_s(z) = \frac{1}{a} d_s(z/b). \tag{3.7}$$

The solution to (3.7) is determined by direct substitution to be:

$$d_s(z) = A(z)/z^\mu \quad (3.8)$$

where as in (2.4)

$$\mu = \ln a / \ln b \quad (3.9)$$

and

$$A(z) = A(z/b) = \sum_{n=-\infty}^{\infty} A_n \exp[i2\pi n z / \ln b]. \quad (3.10)$$

The solution to (3.7) therefore gives the average diameter as a modulated inverse power-law, since $A(z)$ is a harmonic function in $\ln z$ with period $\ln b$ [West and Goldberger (13); West, Bhargava and Goldberger (12)]. Therefore the multiple scales in the average bronchial diameter should decrease with generation number, not as an exponential, but as a type of modulated inverse power law.

In Fig. 5 we indicate the fit of (3.10) to selected data from Raabe *et al.*, (8) by using a log-log linear regression to compute a slope and intercept and shown by the solid line. The further details of the fitting technique are contained in West *et al.* (12). It is evident that the fractal model captures the essential features of the lung cast data, both qualitatively and quantitatively, thereby vindicating the fractal model of the lung.

From the above consideration we see that the mammalian lung is representative of a fractal structure due to the broad distribution in scales in each generation of the bronchial tree. In addition to this static structure, we also find fractal dynamic processes in physiology. The example considered here is the voltage pulse traversing the His-Purkinje conduction system of the heart [Goldberger, Bhargava, West, and Mandell (3)]. The His-Purkinje system is shown in (Fig. 6) to have a ramified structure which bears a remarkable resemblance to the self-similar bronchial tree. Even here we have conjectured that the repetitive branching of the His-Purkinje system represents a fractal set in which each generation of self-similar sequencing imposes greater and greater detail on the process. At each fork in this network the cardiac impulse activates a new pulse along each conduction branch, thus yielding two pulses for one. In this manner, a single pulse entering the proximal point of the network with N distal branches, will generate N pulses at the interface of the conduction network and the myocardium. Here we see a voltage pulse emanating from the pacemaker nodal region of the heart become shattered into a number of equal amplitude pulses. Each pulse travels a different path length to reach the myocardium and there superimposes to form the classical QRS pulse. The distribution in path lengths resulting from the fractal nature of the branches gives rise to a distribution of decorrelation times τ_c among the individual spikes impinging on the myocardium. The unknown distribution $p(\tau_c)$ can be obtained using an argument parallel to that just used for spatial scales in the lung.

If the correlation function for a single pulse has an exponential form with correlation time τ_c , i.e., $\exp[-t/\tau_c]$, then that constructed for the QRS complex has the form:

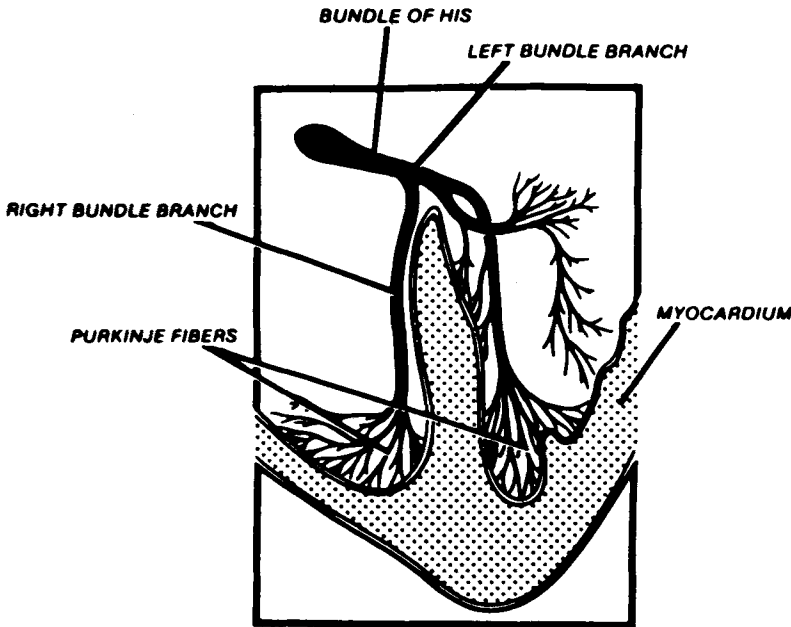


FIGURE 6. The His-Purkinje conduction system of the human heart is sketched.

$$c(t) = \int_0^\infty \exp[-t/\tau_c] p(\tau_c) d\tau_c. \tag{3.11}$$

The correlation time τ_c is referenced to the time to traverse the longest path in the conduction system. This, of course, depends not just on the length of the path, but also on the velocities in each branch which in turn depend on branch diameters. If the path lengths and traversal times are distributed in a scaling fashion with shorter total path lengths and time being rarer, then we use the argument leading to (3.7) by considering a sequence of shorter correlation times τ_c/b each with a small probability $1/a$. Thus, we obtain the RG relation for the correlation function:

$$C(t) = b/a C(bt), \quad a, b > 1. \tag{3.12}$$

The solution to this functional equation is of the form:

$$C(t) = A(t)t^{\mu-1} \tag{3.13}$$

where $\mu = \ln a / \ln b$ and again $A(t)$ is in general a harmonic function in $\ln t$ but with period $\ln b$. The power spectrum $S(\omega)$ for the QRS pulse is obtained by taking the Fourier transform of the correlation function $C(t)$:

$$S(\omega) = \int_{-\infty}^\infty e^{-i\omega t} C(t) dt. \tag{3.14}$$

If $A(t)$ is slowly varying in time or is constant, the integral in (3.14) can be evaluated using a Tauberian Theorem to be:

$$S(\omega) \sim \frac{1}{\omega^\mu}. \tag{3.15}$$

Thus, according to this argument the QRS waveform should have an inverse power-law spectrum. In Fig. 7 is depicted the power spectrum of normal ventricular depolarization (QRS) wave form from 21 healthy men. The dominant behavior is clearly that of an inverse power law. (3)

Here we can draw a number of tentative conclusions:

1. Bronchial architecture is a consequence of nature having selected a structure with no fundamental scale of length.
2. The structure of the His-Purkinje conduction system of the heart is selected for by nature so as to have no fundamental scale of time.

These conclusions force us to ask why nature prefers not to have a scale. Why are fractal structures apparently preferred in biological systems?

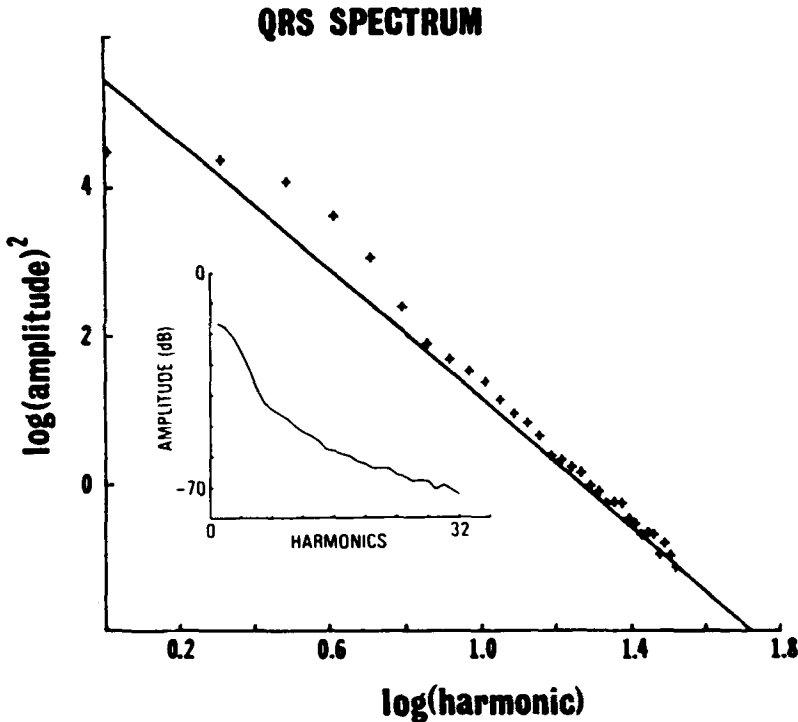


FIGURE 7. The power spectral density of normal depolarization (QRS) waveform from 21 healthy men is shown [from Goldberger *et al.* (3)].

4. TOLERANCES TO FLUCTUATIONS

The two physiological systems we have discussed in some detail clearly suggest that nature may prefer fractal structures to those generated by more traditional scaling. The reason as to why this is the case may be related to the tolerance that fractal structures (processes) seem to possess over and above those of classical structures (processes). Said differently, fractal processes are more adaptive to internal changes and to changes in the environment than are classical ones. Let us construct a simple quantitative model for error response to illustrate the difference between the classical and fractal models (11).

Consider the theoretical average diameter of the lung given by classical scaling, $d(z) = d(0)e^{-\Gamma z}$. Assume that the scaling parameter Γ is made up of two pieces: a constant Γ_0 and a random piece ξ that can arise from random changes in the environment during morphogenesis or from errors in the code generating the structure of the lung. Thus, regardless of whether the errors are produced internally or externally, the average diameter of an airway is given by:

$$\langle d(z) \rangle_\xi = d(0)e^{-\Gamma_0 z} \langle e^{-\xi z} \rangle_\xi, \tag{4.1}$$

where $\langle \rangle_\xi$ denotes an average over an ensemble of realizations of the ξ -fluctuations. To evaluate this average we must specify the statistics of the ξ -ensemble. For convenience we assume ξ is a zero-centered, Gaussian random variable with $\xi = 0$ and $\sigma^2 = \xi^2$. Thus, (4.1) is evaluated to be:

$$\langle d(z) \rangle_\xi = d(0)e^{-\Gamma_0 z} e^{\sigma^2 z^2 / 2} \tag{4.2}$$

so the error grows as $e^{\sigma^2 z^2 / 2}$. The assumed statistics for ξ have no significance except that they provide a specific functional form for the error that can be used to compare the classical and fractal models.

In the fractal model of the lung let us assume that the power-law index consists of two pieces: a constant piece μ_0 and a random piece ξ . Here again the average diameter is averaged over the ξ -fluctuations

$$\langle d(z) \rangle_\xi = \frac{A(z)}{z^{\mu_0}} \langle e^{-\xi \ln z} \rangle_\xi. \tag{4.3}$$

Again using a zero-centered Gaussian distribution to evaluate the ξ -average we obtain:

$$\langle d(z) \rangle_\xi = \frac{A(z)}{z^{\mu_0}} \exp[\sigma^2 (\ln z)^2 / 2] \tag{4.4}$$

so that the error in the fractal model grows as $\exp[\sigma^2 (\ln z)^2 / 2]$.

We define the error generated in the average diameter in either model as:

$$\epsilon_j(z) \equiv \langle d(z) \rangle / d(z)_j \tag{4.5}$$

where $j = c, f$ and $d(z)_j$ denotes the average diameter in the absence of error for the classical (c) and fractal (f) model. In Fig. 8 we graph $\epsilon_j(z)$ for both the classical

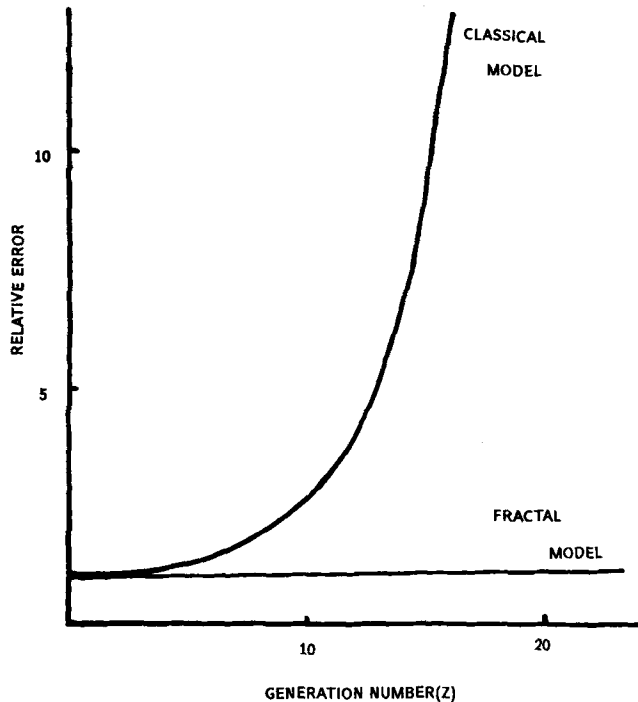


FIGURE 8. The error between the model prediction and that prediction with a noisy parameter is shown for the classical scaling model and the fractal model [from West (11)].

and fractal models. We see that the classical model propagates error in an exponential way, so that by the twelfth or thirteenth generation, the predicted size of the airway with and without error differs by a factor of five. An organism with this sensitivity to error (or to fluctuations in the environment during morphogenesis) would not survive over many generations of the species.

On the other hand we see that the fractal model is essentially unresponsive to error; it is very tolerant of the variability in the physiological environment. It is evident that this error tolerance can be associated with the renormalized distribution of scales constructed in the preceding section. This distribution ascribes many scales to each generation in the bronchial tree, therefore any scale introduced by the error is already present, or nearly so, in the original system. Thus the fractal model pre-adapts the mammalian lung to certain genetic errors and variations in the growth environment.

We may now draw two more tentative conclusions:

3. The modulated inverse power law describes systems that are more error-tolerant than those described by classical scaling.
4. The lack of favored scales promotes the tolerance of variability in physiological systems and favors fractal structures and processes.

5. CONCLUSION

We have discussed two physiological examples in some detail, the mammalian lung and the His-Purkinje conduction system of the heart. In both cases we implement a renormalization argument to obtain an observed inverse power law (as well as the harmonic modulation). From this discussion we infer that inverse power laws often suggest underlying fractal phenomena. In turn the phenomena may well be fractal because of the tolerance of such structures and processes to variability.

REFERENCES

1. Berry, M.V.; Lewis, A.V. On the Weierstrass-Mandelbrot fractal function. *Proc. Roy. Soc. Lond.* 370A:459-484; 1980.
2. Goldberger, A.L.; West, B.J. Fractals in physiology and medicine. *Yale J. Biol. Med.* 60:421-435; 1987.
3. Goldberger, A.L.; Bhargava, V.; West, B.J.; Mandell, A.J. On a mechanism of cardiac electrical stability; the fractal hypothesis. *Biophys. J.* 48:525-528; 1985.
4. Hughes, E.D., Montroll, E.W.; Shlesinger, M.F. *J. Stat. Phys.* 28:111; 1982.
5. Koslow, S.H.; Mandell, A.J.; Shlesinger, M.F., eds. *Perspectives in biological dynamics and theoretical medicine*. New York: New York Acad. Sci; 1987.
6. Mandelbrot, B.B. *Fractals, form and chance*. W.H. Freeman; 1977; *The fractal geometry of nature*. W.H. Freeman; 1982.
7. Montroll, E.W. and Shlesinger, M.F., *Proc. Natl. Acad. Sci.* 79:337; 1982.
8. Raabe, O.G.; Yeh, M.C.; Schum, G.M.; Phalen, R.F. *Tracheobronchial geometry; human, dog, rat, hamster*. Albuquerque, NM: Lovelace Foundation for Medical Education and Research; 1976.
9. Thompson, D.W. *On growth and form*, 2nd Ed.. Cambridge, England: Cambridge University Press; 1963; original 1917.
10. Weibel, E.R.; Gomez, D.M. The architecture of the human lung. *Sci.* 137:577; 1962.
11. West, B.J. In: Kelso, J.A.S.; Mandell, A.J.; Shlesinger, M.F., eds. *Dynamic patterns in complex systems*. Singapore: World Science; 1988.
12. West, B.J.; Bhargava V., Goldberger, A.L. Beyond the principle of similitude: Renormalization in the bronchial tree. *J. Appl. Physiol.* 60:188-197; 1986.
13. West, B.J.; Goldberger, A.L. *Physiology in fractal dimensions*. *Am. Sci.* 75:354-365; 1987.
14. West, B.J.; Goldberger, A.L.; Rovner, G.; Bhargava, V. Nonlinear dynamics of the heartbeat I. The AV junction: Passive conduit or active oscillator? *Physica* 17D:198-206; 1985.